INSTITUTO SUPERIOR DE ENGENHARIA DO PORTO
MESTRADO EM ENERGIAS SUSTENTÁVEIS




Tanger Wind Farm Summary of Site Verification Study

ALEKSANDRA ROGALSKA
Fevereiro de 2017

POLITÉCNICO
DO PORTO

Instituto Superior de Engenharia do Porto

P.PORTO

Politechnika Wrocławska
Wydział Mechaniczno-Energetyczny

ERASMUS PROJECT

Tanger Wind Farm
Summary of Site Verification Study

Student**: Aleksandra Rogalska**
Student number**: 1160166**

Tutor: **PhD. Carlos Silva Santos**

Porto, February 2017

Table of contents

1. Introduction

1.1. Purpose

The present report presents the results for Site Verification Study for the Tanger Wind Farm in Morocco.

The purpose of this study was to estimate a set of relevant wind and climate conditions, external wind conditions and the relevant turbine site and hub height. For the research available climate observation and CFD modelling of wind conditions made by WINDIE™.

1.2. Megajoule – company profile

The goal of the project is to connect both industry and academic approach. The methodology and software used in this project is the same like in the Megajoule company. The typical industry report is enriched by some theoretical knowledge.

Founded in 2004, MEGAJOULE is a privately owned Portuguese company, dedicated to renewable energy consultancy and leader in wind resource assessment in Portugal, one of the leading European markets of wind energy.

MEGAJOULE services cover a wide range of topics related to wind resource assessment, from site evaluation to wind resource assessment studies, including planning and conducting wind measurement campaigns and project due-diligence. Acting globally, MEGAJOULE provides not only wind consultancy but also advice on solar energy and biomass projects.

MEGAJOULE is pleased having some of the biggest project developers, investors, turbine manufacturers and banks as clients in Portugal, as well as having the confidence of several international companies.

1.3. Software

The software used for preprocessing, calculations and postprocessing is WINDIE™. It is a computational fluid dynamics code developed by the group of researchers from the Insituto Superior de Engenharia do Porto. The development was led by Prof. Fernando Aristides Castro who has nearly 20 years of experience in the field of CFD modelling of atmospheric flows applied to the wind industry.

2. Project description and input data

2.1. General location

The wind farm is located in the north of Morocco, just a few kilometers from the Strait of Gibraltar and about 20 km from the Tanger city. Below maps show exact position of Wind Farm.

Figure 2.1 – General location of Tanger wind farm

Figure 2.2 – General location of Tanger wind farm (zoomed)

The area is topographically complexed. It is a mountainous terrain with sea in the neighbourhood. The complexity of the terrain makes that simulation of real wind flow challenging and typical software used in the wind energy industry could give different results than the real wind flow. The altitude of reference point is 232m. Because land cover around the wind farm does not include any forest the canopy module will be neglected in the calculations. It is the region on the top of the mountain so no buildings are considered.

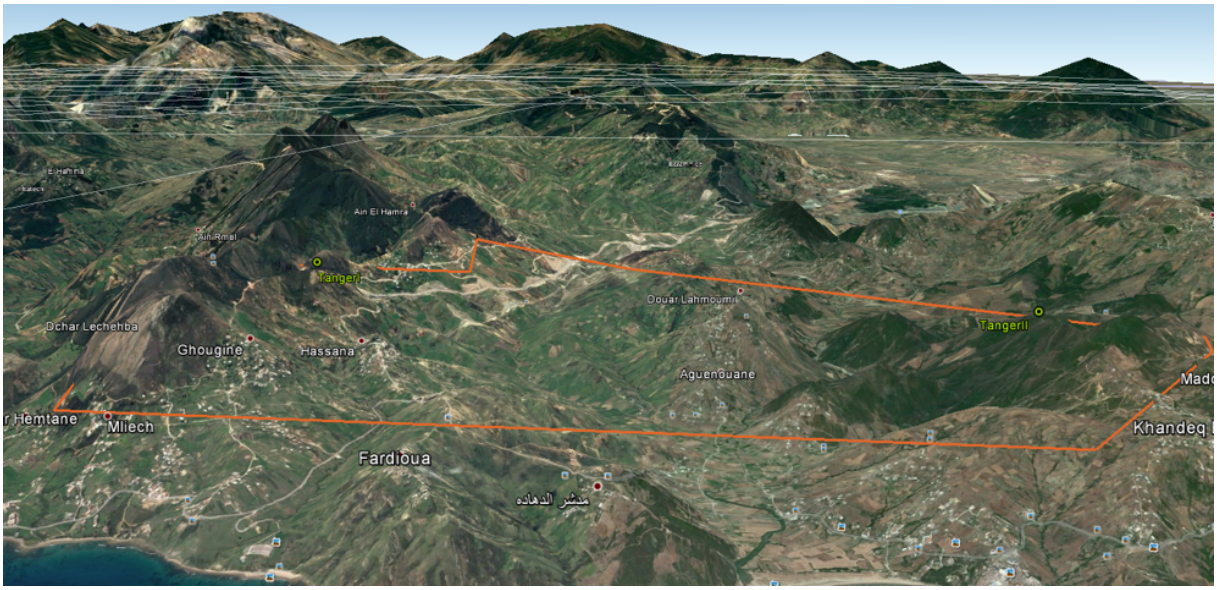

Figure 2.3 – Topographical features of the wind farm

2.2. Wind farm

The following table summarises planned configuration of the Tanger wind farm. One layout will be analyzed. Masts and turbines are planned to be on the top of the mountains. The following pictures indicate where the masts (Tanger 1 and Tanger 2) and turbines (G1-G20) are planned to be installed. The Wind Farm is divided in two parts. On the right side there will be one mast and 13 turbines, and the left side of the picture another mast and 7 turbines.

Table 2.1 – Planned Wind Farm Layout

Nº for WTs	Tubrine model	Hub height [m]	Wind Class
20 (1-20)	Gamesa 128	81	IIA

Figure 2.4 – Turbines and mast-planned layout

Figure 2.5 – Gamesa128 Turbines

2.3. Wind Assessment and Wind Data

A wind assessment campaign has been carried out for this site with the installation since June 2011 to June 2012. Wind data series and information about masts and measurements were supplied. It is assumed that the calibration parameters of the anemometers were correctly applied along the measurement campaigns.

2.4. Input orography, roughness and land cover data.

The topography information and terrain roughness map were supplied.

The topography does not include any forest therefore the canopy module is neglected in the calculations.

3. Methodology

3.1. WINDIE™ wind flow modelling approach

WINDIE™ is a non-linear model that solves the Reynolds-averaged Navier-Stokes equations (RaNS), on terrain-following meshes. WINDIE™ follows a more realistic approach than a linear model or a standard CFD. It can capture complex phenomena such as flow separation, turbulence induced by complex topography, thermal effects, large flow deviations and shear, influence of neighbouring forested areas and other flow features.

WINDIE™ includes a number of turbulence models. In this study two of them were used: k-ε two equation model and tke turbulence kinetic energy model.

WINDIE™ distinguishes from other CFD tools used in the industry because it takes into consideration more facts that other software, for example:

a) it incorporates forest canopy model
b) it is possible to simulate time-dependent simulation using URaNS formulation (Unsteady RaNS)
c) it can be coupled with mesoscale simulations to improve the quality of its results by using boundary conditions which are more representative of local conditions.

Traditional CFD software in wind industry in most cases has an impact for results simplification. Typically the wind flow is just injected with constant direction at one end of the computational domain and has some theoretical velocity profile. What is important no wind is allowed to flow across the top or lateral domain boundaries. The result is wind pattern which rarely occurs in real conditions. To minimize the impact of these simplification on the results large domains are used in most cases. It is done to enforce some distance between domain boundaries to give enough space for the wind flow to become more like in real condition. However, the results could still differ from real local winds.

In WINDIE™ this simplification is removed and replaced by using three-dimensional wind fields obtained be mesoscale simulations over a large area around the wind farm. Because of that, the effect of surrounding topography modelled by the WRF mesoscale model has impact on boundary conditions. The flow is allowed to enter and leave any boundary and theoretical profiles are not imposed.

3.2. Synthesis with local wind observation

12 simulations were done (from 0 degree to 330 every 30 degree). Once they are completed the synthesis process should be conducted to check the quality of calculations by checking the validation error.

A transfer matrix which relates measured velocities and turbulence to the values calculated by WINDIE™ at any relevant position inside the domain (turbine or mast) and height above the ground in the wind farm.

Velocity values are synthesized by equation below. The synthesis procedure is the sum of this equation, one for each transported quantity.

$$\hat{V}_h^i = \frac{\tilde{V}_h^i}{\tilde{V}_h^*} \cdot V_h^*$$

Where:

$\hat{V}_h^i$ - synthesised value

$\sim$ indicates calculated quantities

$*$ refers to reference station

i identifies the target point where the synthesis is being performed

V_h^* is measurement velocity collected at the reference station

Turbulence values are synthesised by the formula below.

$$I^{\wedge}{}_{u}^{i} = I^{\sim}{}_{u}^{i} + \Delta I_u * \frac{V^{\sim}{}_{h}^{*}}{V^{\sim}{}_{h}^{i}}$$

Where:

$\Delta I_u = I_u^* - I^{\sim}{}_u^*$ is the difference between the measurement and calculated horizontal turbulence

All the values description is analogical like for the equation above for the velocity.

All typical statistics often used in wind data analysis can be calculated from the synthesised value. The synthesis can be applied to wind speed and direction frequency histograms, wind roses, mean turbulence and turbulence standard deviation and extreme value extrapolation.

3.3. Assessment of numerical results

Verification of the model behavior for each model should be performed. There are two types of cross estimates which should be done:

- horizontal cross prediction – between available masts
- vertical cross prediction – between available measurements heights.

3.4. Air density correction of wind speed

It is recommended to take into consideration the change of wind speed value depending on changing density with height. In this cases wind farm is quite high above the sea level. To get real value of wind speed it should be calculated with formula:

$$V^* = V\sqrt[3]{\frac{\rho}{1.225}}$$

Where:

V^* is the corrected wind speed value
V is original wind speed value
ρ is the average annual air density defined for the site.

Below is the part of the WINDIE™ code for air density correction.

```
# AIR DENSITY CORRECTION
t0        = 291.65                          # reference temperature [K]
p0        = 99000.0                         # reference pressure    [Pa]
z0        = 232.0                           # altitude of reference point [m]
B         = 0.0065                          # lapse rate [K/m] (use +ve value)
```

Figure 3.1 WINDIE™ air density correction

3.5. Annual average temperature

Annual average temperature and pressure were taken from NASA website for proper longitude and latitude. Values are shown it the picture 3.1. These values are the averages from many years of NASA measurements.

3.6. Turbulence model

a) k-ε

In the calculations the basic turbulence model was k-ε.

K-epsilon (k-ε) turbulence model is the most common model used in Computational Fluid Dynamics to simulate mean flow characteristics for turbulent flow conditions. It is a two equations model which gives a general description of turbulence by means of two transport equations (PDEs). Two equation model means that it includes two extra transport equations to represent the turbulence properties of the flow. The first variable is turbulence kinetic energy 'k'. It determines the energy in the turbulence. The second variable is turbulent dissipation 'ε'. It determines the scale of turbulence. Mostly, k-ε model should be used for free-shear layer flows with relatively small pressure gradient. The model gives good results for the cases where mean pressure gradients are small. Accuracy could be reduced for flows containing large adverse pressure gradients. K-epsilon model might be an inappropriate turbulence model for problems such as inlets and compressors.

Tanger wind farm is at the top of the mountains. The chosen turbulence model should have the ability to show real flow even with complex orography. According to Castro work [6] limitation of the k-epsilon model is the negative shear stress above

the hilltop. Other important aspects are the effect of the constant roughness length, steady state flow assumptions and also the possible impact of neighbouring hills downstream. It is worth to indicate that upstream of the hilltop k was overpredicted. That was attributed to modelling limitations of the production term and the inability of the k− ε model to accommodate the effects of the streamline curvature.
Castro says that for locations closer to the hilltop, the reduction in the characteristic roughness improved the agreement between the numerical and the experimental data in the vertical profiles, both of k and speed-up at ht and cp.
The conclusion of the simulations carried in Castro research was that the nearby hills did not affect the flow at the top or downstream the hill (Askervein Hill research).

a) TKE 1.5 turbulence model

The turbulence model used in calculations originates from the WRF modelling system (Weather Research and Forecasting). It is a model which has a transport equation for the turbulent kinetic energy and additional expressions (not transport equations) to calculate the production and dissipation of the turbulence kinetic energy as well as buyoancy terms if needed. The prognostic equation governing the evolution of the turbulent kinetic energy e is:

$$\partial_t(\mu_d e) + (\nabla \cdot V_e)_\eta = \mu_d(\text{shear production} + \text{buoyancy} + \text{dissipation})$$

The time integration and the transport terms in the above equation are integrated in the same manner as for other scalars. The right-hand side source and sink terms for e are given as follows.

Shear Production

The shear production term can be written as

$$\text{Shear production} = K_h D_{11}^2 + K_h D_{22}^2 + K_v D_{33}^2 + K_h \overline{D_{12}^2}^{xy} + K_v \overline{D_{13}^2}^{x\eta} + K_v \overline{D_{23}^2}^{y\eta}.$$

Buoyancy

The buoyancy term in the TKE equation is written as

$$\text{Bouyancy} = -K_\upsilon N^2,$$

where the Brunt-Vaisala frequency N is computed using either the formula for a moist saturated or unsaturated environment:

$$N^2 = g\left[A\frac{\partial \theta_e}{\partial z} - \frac{\partial q_w}{\partial z}\right] \text{ if } q_v \geq q_s \text{ or } q_c \geq 0.01 \text{ g/Kg};$$
$$N^2 = g\left[\frac{1}{\theta}\frac{\partial \theta}{\partial z} + 1.61\frac{\partial q_v}{\partial z} - \frac{\partial q_w}{\partial z}\right] \text{ if } q_v < q_s \text{ or } q_c < 0.01 \text{ g/Kg}.$$

The coefficient A is defined as

$$A = \theta^{-1}\frac{1 + \frac{1.61\epsilon L q_{vs}}{R_d T}}{1 + \frac{\epsilon L^2 q_v}{C_p R_v T^2}},$$

where qw represents the total water (vapor + all liquid species + all ice species), L is the latent heat of condensation and ϵ is the molecular weight of water over the molecular weight of dry air. θ_e is the equivalent potential temperature and is defined as

$$\theta_e = \theta\left(1 + \frac{\epsilon L q_{vs}}{C_p T}\right),$$

where qvs is the saturation vapor mixing ratio.

Dissipation

If Δ_x is less than the critical length scale lcr, the dissipation term is

Dissipation = $-\frac{Ce^{3/2}}{l}$,

where

$$C = 1.9C_k + \frac{(0.93 - 1.9C_k)l}{\Delta_s},$$

$\Delta_s = (\Delta_x\Delta_y\Delta_z)^{1/3}$, *and* $l = \min\left[\left(\Delta_x\Delta_y\Delta_z\right)^{\frac{1}{3}}, 0.76\sqrt{e}/N\right]$.

If Δ_x is greater than the critical length scale lcr, the dissipation term is

dissipation = $-\frac{2\sqrt{2}e^{\frac{3}{2}}}{15l}$,

where $l = \frac{kz}{1+kz/l_0}$,

$$l_0 = \min\left(\frac{\propto_b \int_0^{z_i}\sqrt{ez}dz}{\int_0^{z_i}\sqrt{e}dz}, 80\right)$$

$\propto_b$= 0.2, and k = 0.4 is the von Karman constant.

4. Results

4.1. Local wind data

The local wind data was supplied. Available data was for 20, 40 and 60 meters for both masts. The supplied data is free from errors.

4.2. Long term adjustment and reference wind data

In order to obtain reliable characteristics for the wind it is recommended to use wind data series from as many years as possible. In order to get reliable wind data measurements the period from 10-20 years should be considered. It helps to avoid gaps of missing and rejected data, reduce the inner-annual variability and make sure that the data of the project is not an anomaly with for example one very windy year. For discussed wind farm it was 11 years period (from June 2001 to June 2012).

The MCP correlation is used to evaluate the integrity of data mutual connection. It is evaluated by examination of sectorwise wind speed correlation and by self-consistency test. The MPC correlation is applied to the measurement period and compared with collected data.

The MCP correlation is based on:

a) sectorwise correlation of hourly average wind speed for twelve 30° sectors for concurrent site and reference datasets;
b) veer correction by means of a veer correction matrix between site and reference datasets;
c) extrapolation of intended data periods from reference datasets by use of above transfer functions between wind speed and direction.

The results of self-consistency test could be shown as the local wind rose and wind speed frequency histogram for the correlated data. The following pictures present wind rose and speed frequency histogram for discussed wind farm for 11 years for both masts (tan1 and tan2). All of the results of the self-consistency test can be found in Appendix.

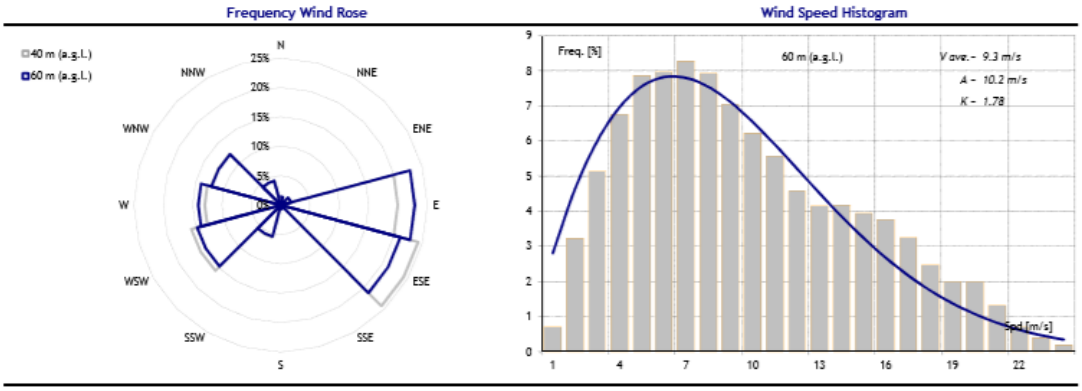

Figure 4.1 – Wind rose and wind speed frequency histogram for TAN 1, 11 years data, June 2001-June 2012

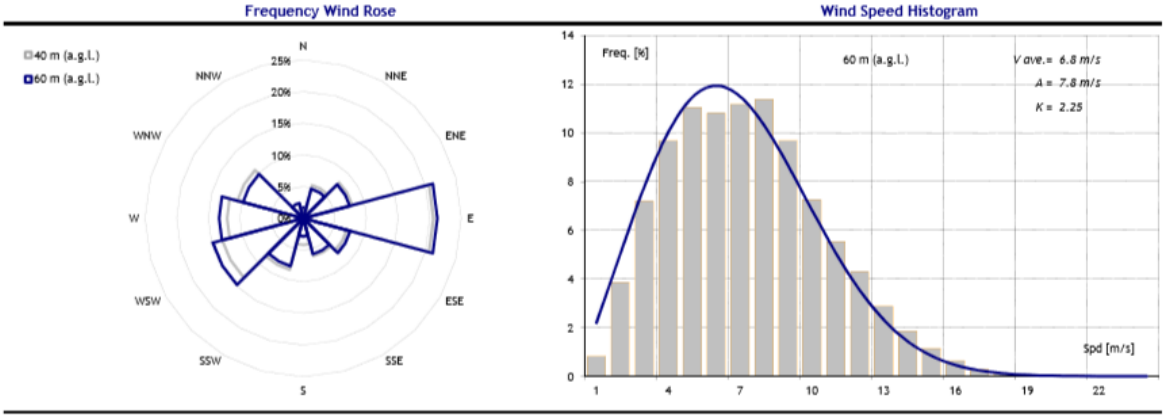

Figure 4.2 – Wind rose and wind speed frequency histogram for TAN 2, 11 years data, June 2001-June 2012

4.3. Extreme value extrapolation (V_{ref} and V_{e50})

The extrapolation of extreme is based on finding the values of 10 min wind speed averages (V_{ref}) and 3 seconds gust (V_{e50}) considering the next 50 years. The process is based on the Independent Storm Method. The sample of relevant independent maxima is selected for each data series. The goal of the sampling is to find maximum values in 7 days time-window above a given threshold. Such a long time window is used to avoid dependence from the synoptic event.

Threshold is the function of number of maximum events selected versus the calculated statistical uncertainty of the Paretto distribution fit.

The resultant sample of extremes is fitted with the Paretto distribution.

The results of the extreme wind analysis and extrapolation for V_{ref} and V_{e50} for the Tanger Wind Farm are summarised in the following table. Please note that the wind speed values on these tables are not air density corrected.

Table 4.1 – Summary of V_{ref} extrapolation for TAN1 and TAN2 masts

Mast	Wind Data Period	Threshold [m/s]	Time Window [days]	No. Of Samples of Extremes (10 min. Averages)	Vref (50 year maximum) [m/s]	Statistical uncertainty of fitted distribustion [m/s]
TAN1	Jun11-Jun12	23,2	7	10	30,76	2,42
TAN2	Jun11-Jun12	23,2	7	10	30,76	2,42

Table 4.2 – Summary of V_{e50} extrapolation for TAN1 and TAN2 masts

Mast	Wind Data Period	Threshold [m/s]	Time Window [days]	No. Of Samples of Extremes (10 min. Averages)	Vref (50 year maximum) [m/s]	Statistical uncertainty of fitted distribustion [m/s]
TAN1	Jun11-Jun12	28,4	7	11	43,95	4,75
TAN2	Jun11-Jun12	28,4	7	11	43,95	4,75

4.4. Mesh

A proper mesh is one of the most important factors which has influence on right results.

It is observed that in a square of dxn, dyn (in the middle) there is larger density of control volumes. It calls high resolution area where control volumes have dimensions cofx by cofy. Then the cells start expanding. The following picture explains all the important mesh parameters and shows mesh used to the calculation in the final case.

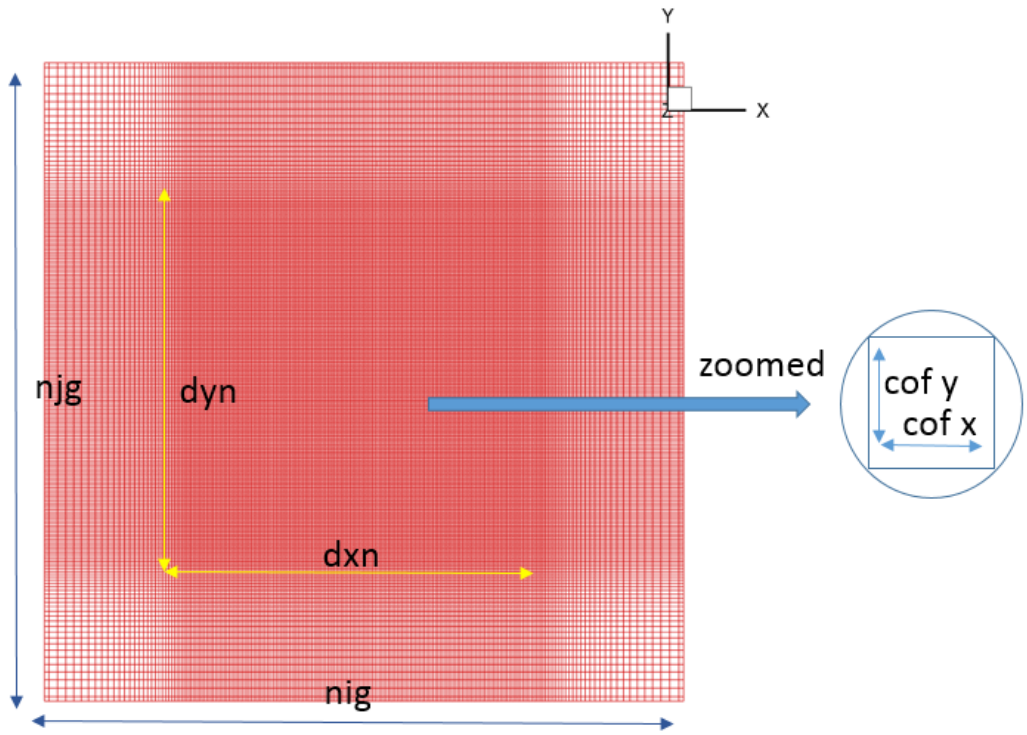

Figure 4.3 – Mesh view from above

Below the mesh view from the side. Zoomed two times to show first layers near the ground. 'Cof z' is the distance from the center of first cell to the ground.

Vertically, the mesh is concentrated near the ground (Figure 4.4.) due to more complex wind flow close to the ground than above. To simulate actual air flow, considering that effect of viscosity near the ground is significant, proper boundary layer should be done (Figure 4.4).

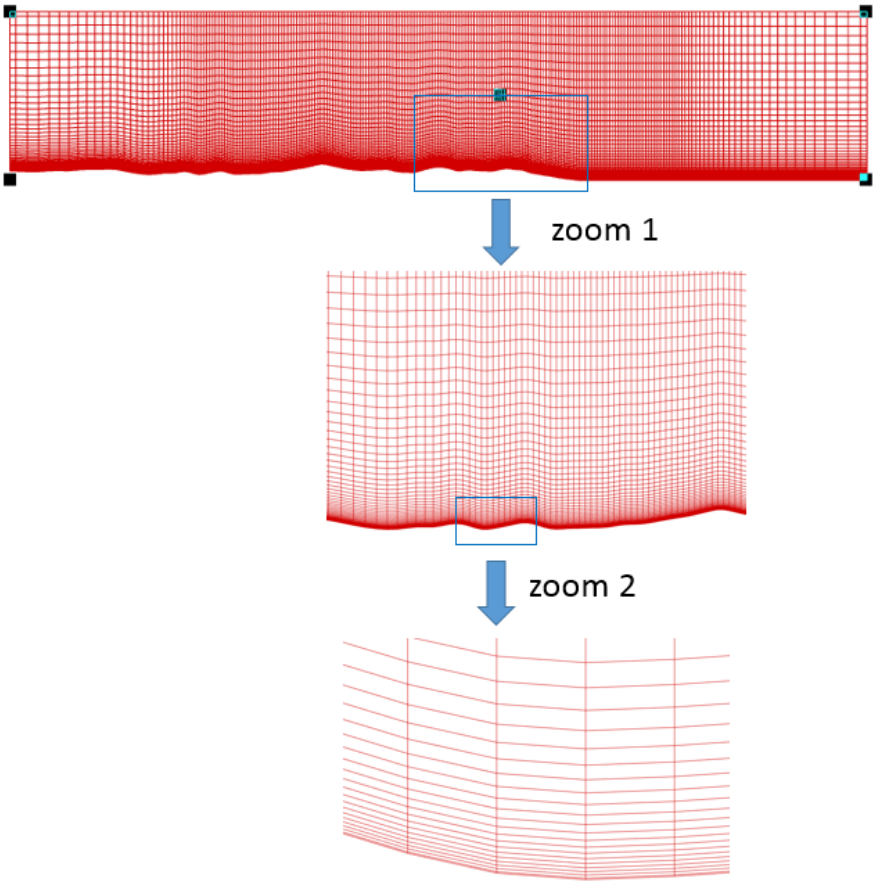

Figure 4.4 – Mesh view from the side - zoom for boundary layer

4.5. CFD model configuration

In this particular case the orographic complexity demanded a few sets of simulations before the best one was found. In the final case desired convergence criteria were met and model performance was fine-tuned. Every set of simulations differ with the quality of mesh (dxn, dyn, dzn parameters), meshed area or turbulence model. The final set contain 12 simulations (from 000 degree to 330 degree every 30 deg.) which were used to the synthesis procedure. The table below shows used parameters.

Table 4.3 – Windie™ CFD configuration of final direction simulations

Dir [°]	Mesh area [km2]	Central points [WGS84 UTM35S, M]	Mesh refinement area	ni	nj	nk	Horisontal resolution [m]	Heigth first vertical node [m]	Forest Model	Coriolis	Couplin Mesoscale
000	519,84	262411.5, 3964565.0	12700x12700	218	218	55	80	2	NO	YES	NO
030	519,84	262411.5, 3964565.0	12700x12700	218	218	55	80	2			
060	519,84	262411.5, 3964565.0	12700x12700	218	218	55	80	2			
090	519,84	262411.5, 3964565.0	12700x12700	218	218	55	80	2			
120	519,84	262411.5, 3964565.0	12700x12700	218	218	55	80	2			
150	519,84	262411.5, 3964565.0	12700x12700	218	218	55	80	2			
180	519,84	262411.5, 3964565.0	12700x12700	218	218	55	80	2			
210	519,84	262411.5, 3964565.0	12700x12700	218	218	55	80	2			
240	519,84	262411.5, 3964565.0	12700x12700	218	218	55	80	2			
270	519,84	262411.5, 3964565.0	12700x12700	218	218	55	80	2			
300	519,84	262411.5, 3964565.0	12700x12700	218	218	55	80	2			
330	519,84	262411.5, 3964565.0	12700x12700	218	218	55	80	2			

4.6. Other grid configurations

Before the final parameters were found a few meshes were considered. Four first runs had the same mesh area differing just with the quality of the mesh. Regardless the modifications of mesh parameters, horizontal cross-prediction error still was too high. It was decided to increase the mesh area and the mesh refinement area for runs 5 and 6. After that change the cross predictions errors were acceptable. A picture below shows the mesh increase. The yellow border limits first proposition of the mesh size, the red line indicates expanded mesh. The new mesh was increased by 500m in each direction.

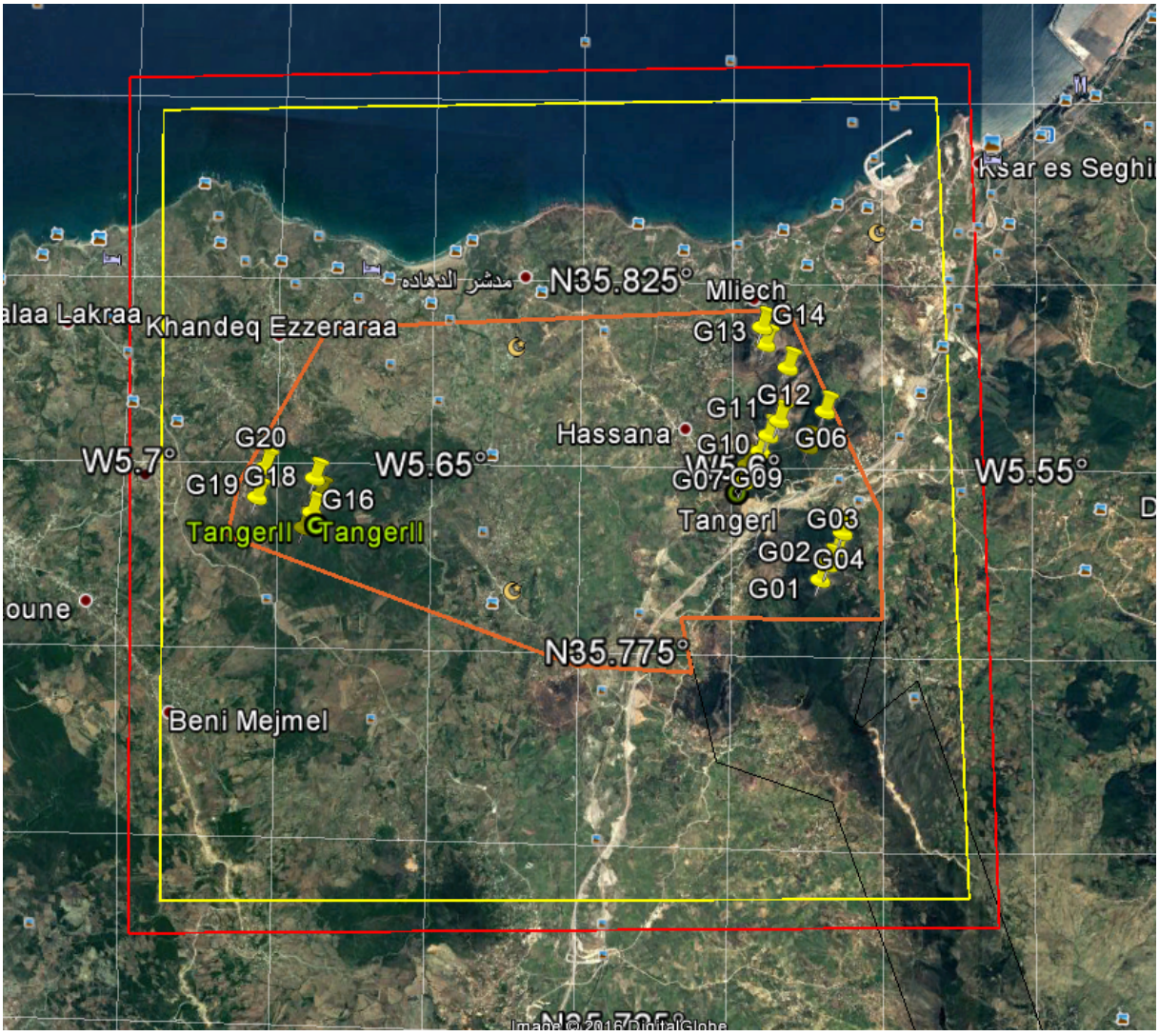

Figure 4.5 The increase of the mesh area

Surprisingly, when the turbulence model for the final case was changed from k-ε to tke the cross-prediction error increased significantly. The error from the validation for tke turbulence model cannot be accepted. The following table shows modification of all the parameters and cross predictions errors for all of the 6 cases. The red border around the run5 indicates the case with the lowest errors. It was called the final case, and all the results in this report refer to that case.

Table 4.4 – The most important parameters for other grid configurations

Case	Mesh area [km2]	Central points [WGS84 UTM35S, M]	Mesh refinement area	ni	nj	nk	Horisontal resolution [m]
run01	473,72	262411.5, 3964565.0	11765x11765	120	120	45	144
run02	473,72	262411.5, 3964565.0	11765x11765	168	168	45	98
run03	473,72	262411.5, 3964565.0	11765x11765	120	120	65	144
run04	473,72	262411.5, 3964565.0	11765x11765	220	220	55	71
run05	519,84	262411.5, 3964565.0	12700x12700	218	218	55	80
run06	519,84	262411.5, 3964565.0	12700x12700	218	218	55	80

Table 4.5 – The most important parameters for other grid configurations - continued

Case	Heigth first vertical node [m]	Forest Model	Coriolis	Couplin Mesoscale	turbulence model	Horisontal cross-prediction error	
						TAN1 to TAN2	TAN2 to TAN1
run01	0,5	NO	YES	NO	k-ε	14,01%	-13,01%
run02	0,5					17,47%	-13,62%
run03	0,5					13,93%	-12,80%
run04	2					4,36%	-8,51%
run05	2					2,88%	-7,09%
run06	2				tke	27,21%	-14,67%

4.7. Assessment of modelling results

The cross-predictions methodology is described in point 3.2.

The following table present the results for the vertical predictions carried out in terms of wind speed and ambient turbulence.

Table 4.6 – Discrepancies between vertical cross predictions and statistical summary (wind speed and turbulence) for TAN1

TAN1, vertical cross-prediction							
		Wind speed [m/s]			TI(V>5) [%]		
From	To	Observed	Estimated	error_Windie	TI_Measured	TI_Estimated	diff TI
20TAN1	40TAN1	9,30	9,41	1,20%	7,69	8,90	1,21%
40TAN1	20TAN1	9,10	8,99	-1,15%	9,12	7,87	-1,25%
20TAN1	60TAN1	9,27	9,59	3,44%	7,36	8,67	1,31%
60TAN1	20TAN1	9,10	8,81	-3,18%	9,12	7,74	-1,38%
40TAN1	60TAN1	9,27	9,47	2,18%	7,36	7,50	0,14%
60TAN1	40TAN1	9,10	9,10	-2,09%	7,69	7,56	-0,13%
				Wind speed			diff IT
	RMS			2,37%			1,06%
	BIAS			0,40%			-0,10%
	STD			2,37%			1,06%

Table 4.7 – Discrepancies between vertical cross predictions and statistical summary (wind speed and turbulence) for TAN2

TAN2, vertical cross-prediction							
		Wind speed [m/s]			TI(V>5) [%]		
From	To	Observed	Estimated	error_Windie	TI_Measured	TI_Estimated	diff TI
20TAN2	40TAN2	6,35	6,71	8,00%	12,68	13,91	1,23%
40TAN2	20TAN2	6,35	6,35	2,00%	14,19	12,84	1,35%
20TAN2	60TAN2	6,85	6,94	1,44%	12,12	13,64	1,52%
60TAN2	20TAN2	6,35	6,28	-1,16%	14,19	12,4	-1,78%
40TAN2	60TAN2	6,85	6,93	1,30%	12,12	12,45	0,33%
60TAN2	40TAN2	6,7	6,62	-1,24%	12,68	12,3	-0,38%
				Wind speed			diff IT
	RMS			3,53%			1,23%
	BIAS			10,34%			2,27%
	STD			3,08%			1,17%

The vertical validations show that wind speed is accurately captured. The errors are ca. 2-3%. WINDIE™ can show even better performance. It is possible to receive RMS error close to 1%, but to achieve that it would be compulsory to improve the mesh again. The RMS errors for TAN1 and TAN1 respectively 2,37% and 3,53% are considered as acceptable.

The turbulence intensity profile also show quite a good performance. The errors in both cases are about 1%.

The following table shows the results for the horizontal cross-predictions. This test is important because predictions between two masts are much more challenging that just between different heights.

The table below presents horizontal cross-predictions results.

Table 4.8 – Discrepancies between vertical cross predictions and statistical summary (wind speed and turbulence) for TAN1 and TAN2 at the height 60m

TAN 1 & TAN2, horizontal cross-prediction							
		Wind speed [m/s]			TI(V>5) [%]		
From	To	Observed	Estimated	error_Windie	TI_Measured	TI_Estimated	diff TI
60TAN1	60TAN2	6,85	7,05	2,88%	12,12	9,47	-2,66%
60TAN2	60TAN1	9,27	8,61	-7,09%	7,36	9,13	1,77%
				Wind speed			diff IT
	RMS			3,12%			1,30%
	BIAS			-4,21%			-0,89%
	STD			4,99%			2,22%

The RMS errors are similar to pervious validations. In terms of wind speed the errors are 2,88% and -7,09% what was the best result from all of the cases. Considering the cross prediction between two masts the result of validation is very good.

4.8. Synthesis with local wind observations

All of the quantities: long term wind distribution for each turbine site, wind frequencies associated with directional Wind Shear and Flow Inclination, turbulence Intensity values, Reference 10-min and 3-sec velocities for 50-years return horizons were calculated from the available 11 years measured data.

Table 4.8 – Wind data used for synthesis

Mast and Height	All SA quanities	Remarks
TAN1 and TAN2 20,40,60m	June 2001- June 2012	All turbines, both masts

4.9. Annual average temperature and air density

Temperature and atmospheric pressure observations were available from the masts TAN1 and TAN2 and were used for the air density at each turbine position. The data was supplied and it is assumed the data is free from errors.

4.10. Annual average wind speed distribution

The following picture shows the map of average wind speed distribution. The long-term-adjustment average wind speed was calculated at hub height 81m using Long-Term data synthesised from both masts. The values presented at the figure are after air-density correction.

Clearly noticeable is the wind speed dependency of the altitude. The higher altitude the higher wind speed distribution can be seen. That is why all the turbines are planned on the top of the mountains. On the map it is clearly visible that the layout of the turbines is well prepared in term of average wind speed. The possible exception could be turbine G05. It

could be considered to install it more to the east. Rest of the turbines seem to be in the right places where the average wind speed is about 8.5 m/s.

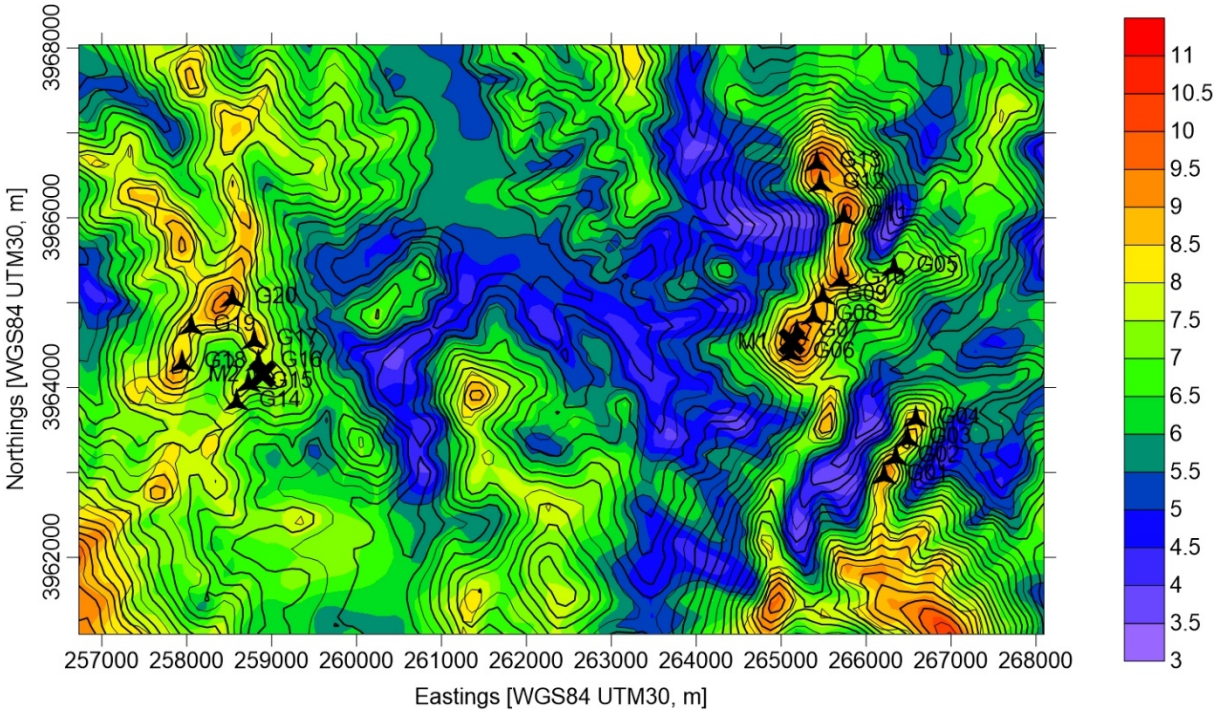

Figure 4.6 Average long-term wind speed at 81 m, includes air density adjustment

4.11. IEC Multi-Layer Maps

Gamesa 128 are turbines planned to install at the wind farm. They have IEC Wind Class IIA. According to IEC 61400-1 a few parameters have to be respected:

- Average Wind Speed at hub height below 8.5 m/s;
- Maximum 50 years 10 min. Wind Speed at hub height (V_{ref}) below 42.5 m/s;
- 360º average Vertical Wind Shear (α) between 0 and 0.2;
- Maximum and Minimum Flow Inclination or Tilt (for 12º sectors) between +/-8º;
- Characteristic Turbulence Intensity (I_{char}) at 15 m/s below 18%.

The following pictures show multi-layer maps for each site parameter individually: average wind speed (Figure 4.7), maximum 50 years 10min wind speed (V_{ref}) (Figure 4.8), average

wind shear (Figure 4.9), flow inclination (Figure 4.10), turbulence intensity at 15m/s (Figure 4.11). These quantities were estimated using the wind dataset for Tanger wind farm at hub height 81m as input. Please note that wind velocities used in the Multi-Layers maps were corrected in terms of air density in the same way like described at point 3.4 .

Each site parameter will be discussed with a corresponding Multi-Layer map. For each map the red area is where conditions at 81m are outside IEC class IIA limits. The white area is where the values are below the limits so the turbines are located in low risk area.

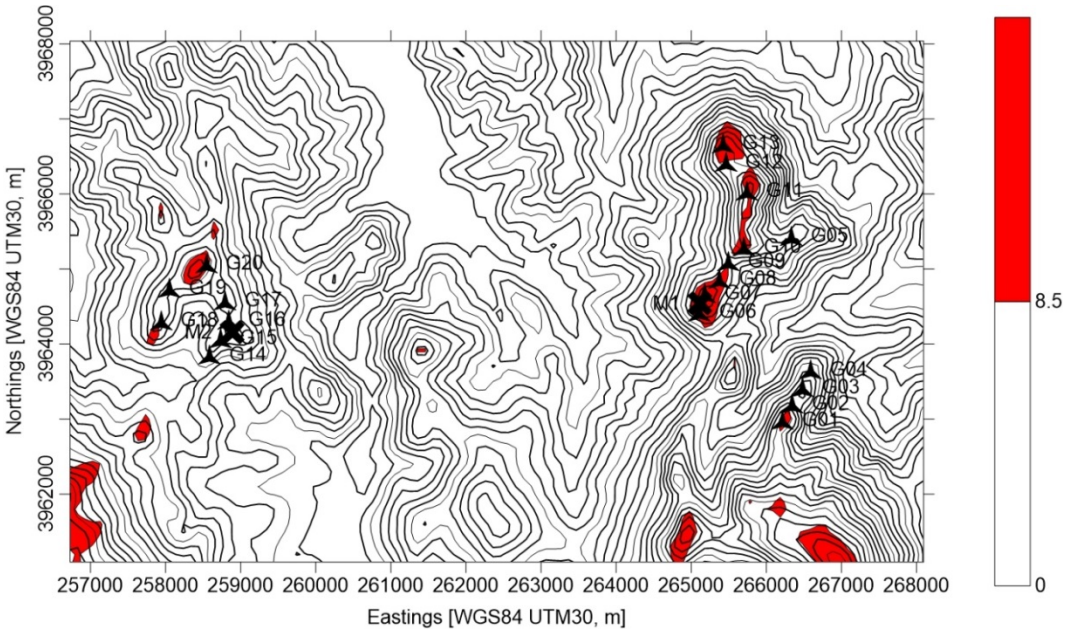

Figure 4.7 Map of area where wind conditions are outside IEC limits for average wind velocity.

The average wind speed for IEC Wind Class IIA should be below 8.5. Figure 4.8 shows that at most of the places where the turbines are planned to be installed average wind speed exceed the limit. For most of the turbines the average wind speed is about 9m/s but for six turbines average wind speed value exceeds 10 m/s (all the values-Table 4.10). In that case it could be considered to install turbines which has Wind Class IA, in which the average wind speed should be below 10m/s. For the turbines with values higher that 10 m/s (G14, G16, G17, G18, G19, G20) it is recommended to do another study for higher speeds than the limit in order to check if the turbines would be installed at the safe area.

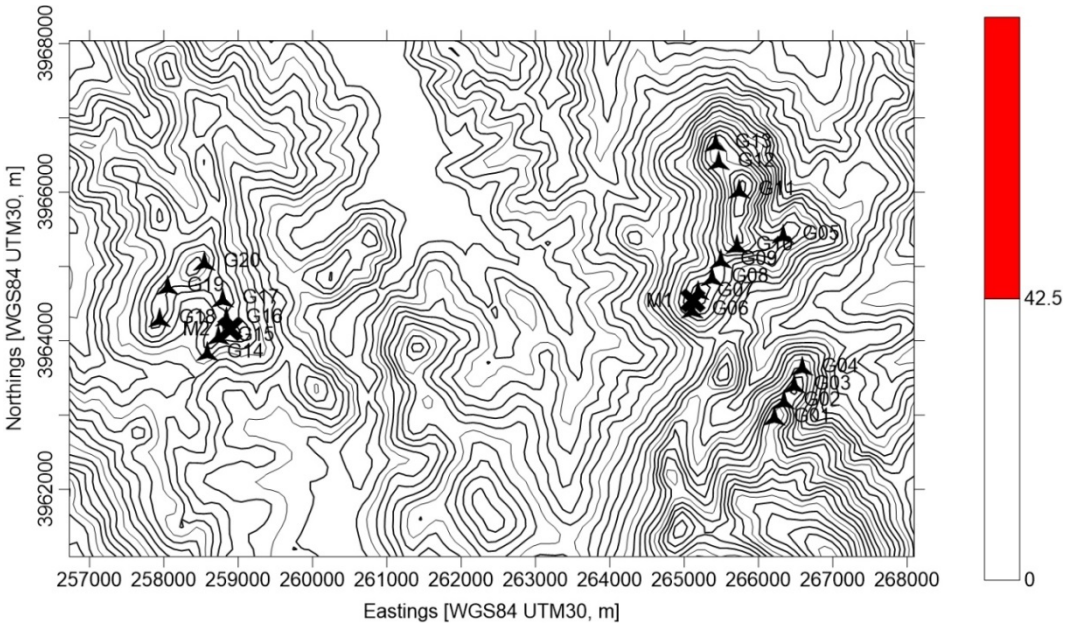

Figure 4.8 Map of area where wind conditions are outside IEC limits for maximum 50 years 10 min. wind speed (V ref)

Seeing that, the multi-layer map is all white, there is no place with high risk area for the wind turbine in terms of maximum 50 years 10 min. wind speed (V ref). This value is below 42,5 m/s in every place of the map.

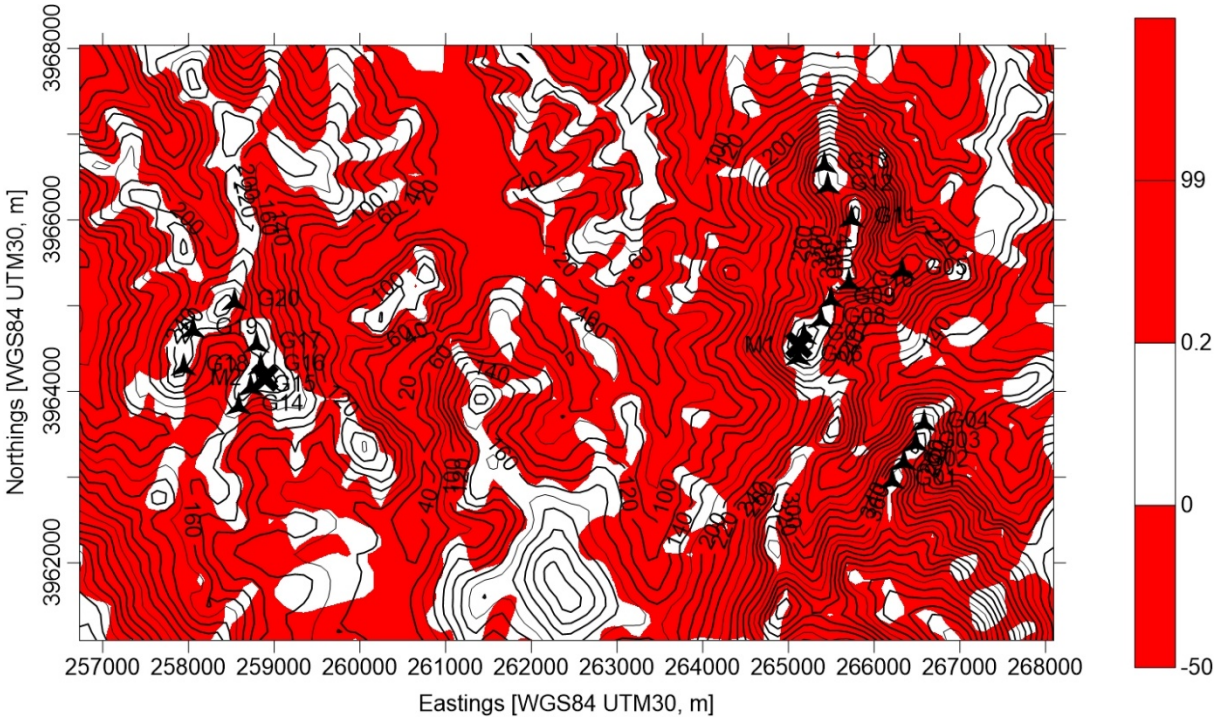

Figure 4.9 Map of area where wind conditions are outside IEC limits shear factor

The map for the shear factor shows that most of the turbines are located at the low risk area. There is one exception, the position of the turbine G05. The predicted shear factor is far too high. While the limit is 0,20, the shear factor for discussed turbine is 0,27. The change of the location of the G05 should be considered. Some of turbines are close to the limit of 0,20 but do not exceed it. That means 19 turbines are located well in terms of shear factor.

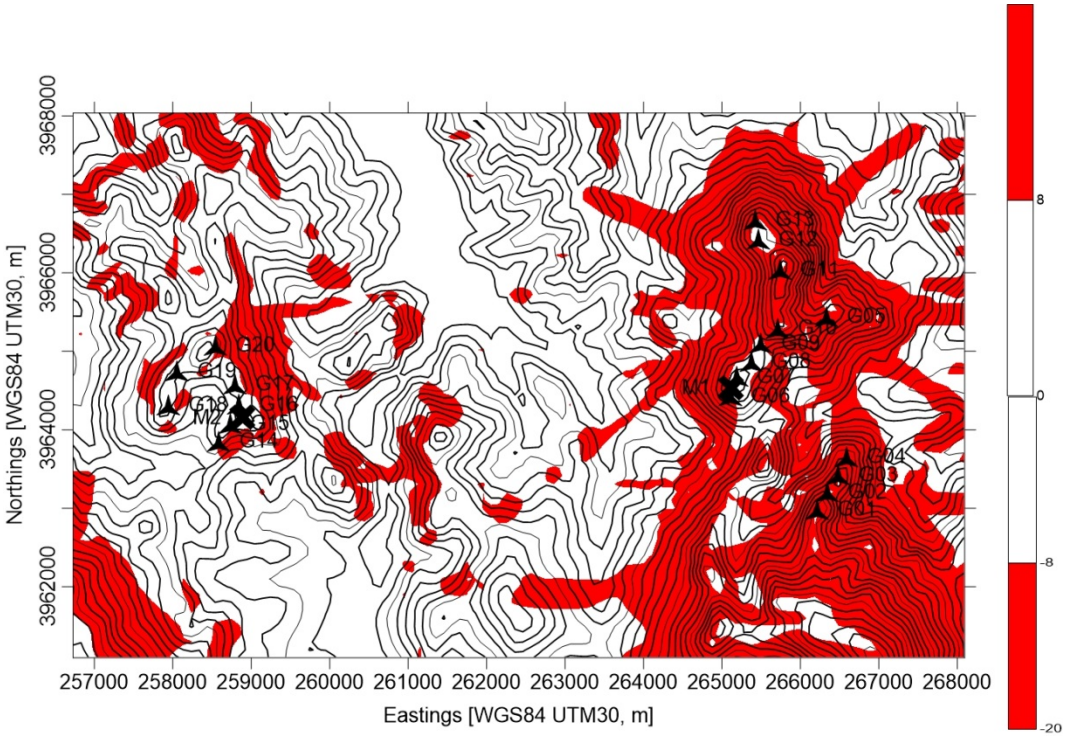

Figure 4.10 Map of area where wind conditions are outside IEC limits for flow inclination

The area where the value of flow inclination is not between -8 and 8 is quite widely spread. However, the only turbines which exceed the limit are G04 (value 12.6) and G13(value 9.1). Especially the location of the turbine G04 should be reconsidered in terms of flow inclination, because now this turbine is at the high risk area.

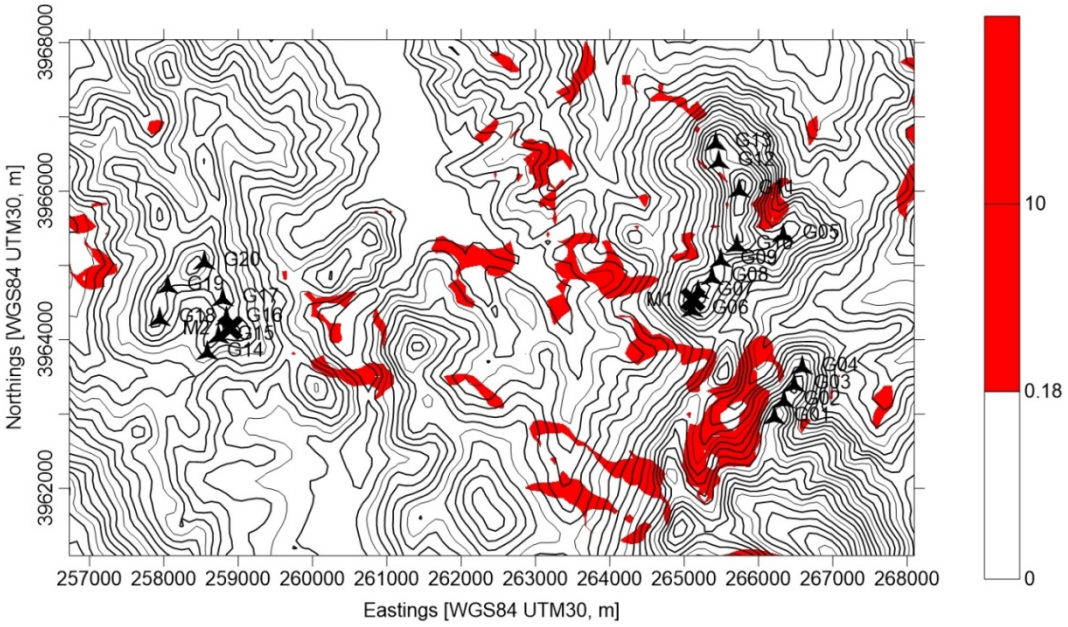

Figure 4.11 Map of area where wind conditions are outside IEC limits for turbulence intensity.

Seeing that, the turbulence intensity for the IEC Wind Class should be below 18%. The figure shows that in every place where the turbines are planned the turbulence intensity is below given limit. It means, that considering turbulence intensity turbines are located at low risk area.

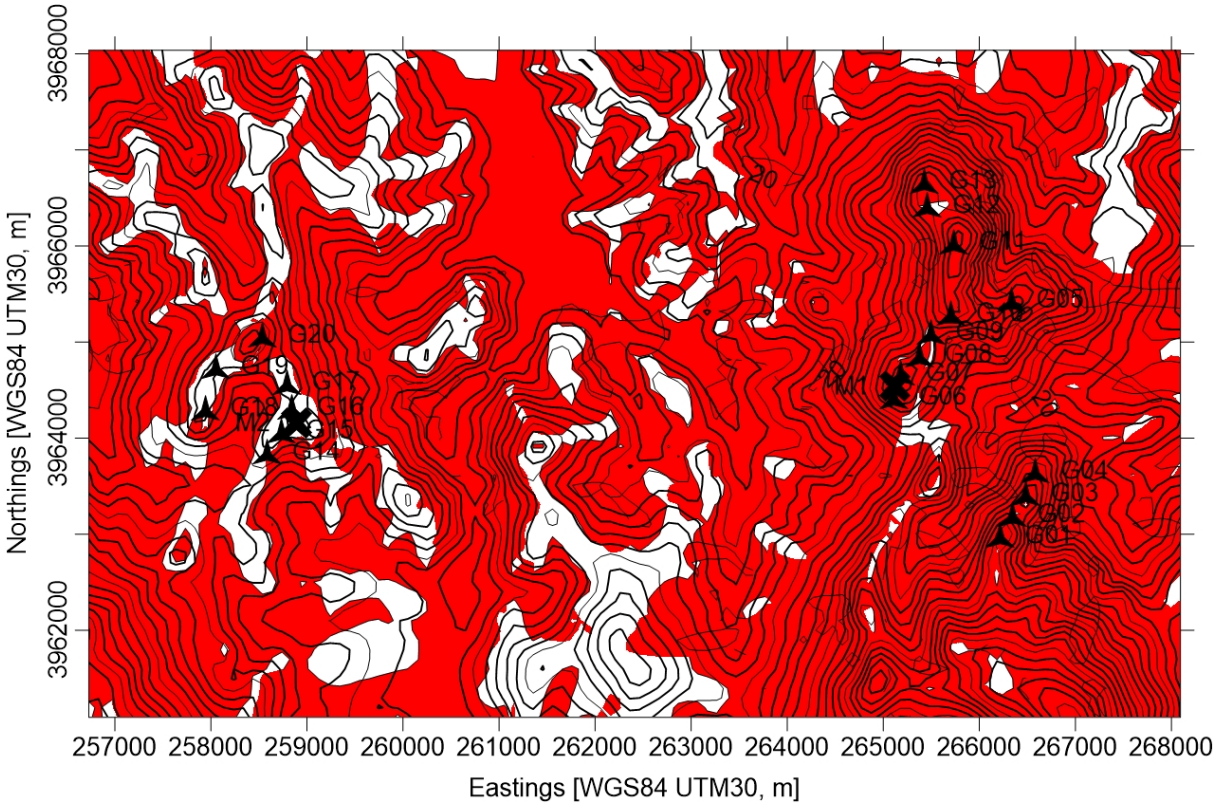

Figure 4.12 Multi-Layer Map of area where wind conditions are outside IEC limits for all the SA parameters.

A map above shows that the area where turbines G01-G13 where planned to be installed in mostly red- high risk areas. Better conditions are seen in the east of the map where the turbines G14-G20 are planned to be installed. Except G20, all of the turbines are at the low risk area. It is suggested to consider IA Wind Class turbines or do load study for chosen turbines (IIA) to make sure that turbines would be installed at enough safe area.

4.12. Site Verification results

The methodology of Site Verification Study is based on the approach that for particular masts suitable turbines are assigned. Thus, for mast one turbines G01-G13 are assigned and for mast two turbines G14-G20 are assigned. The results for each turbines are based on the data for suitable mast.

Table 4.10 – SV Results

Number of turbine (WEC)	Please fill in coordinate system and coordinates. Z (altitude) is the elevation above sea level of the turbine base.			Turbine type	Please see comment	Hub height	Based on long term correlated measurement data / Air density corrected				
WEC	**coordinate system: WGS84 UTM29**			**Type**	**WC**	**HH**	**V_{ave} [m/s]**	**V_{ave-w} [m/s]**	**V_{ref} [m/s]**	**National building code**	**V_{e50} [m/s]**
	X (East)	**Y (North)**	**Z (altitude) [m]**								
G01	266213.0	3962988.0	400.0	G128	IEC	81.0	9.33	N/A	29.95	N/A	42.8
G02	266346.0	3963206.0	334.0	G128	IEC	81.0	8.03	N/A	26.20	N/A	37.4
G03	266485.0	3963423.0	334.5	G128	IEC	81.0	8.64	N/A	27.73	N/A	39.6
G04	266587.0	3963658.0	290.9	G128	IEC	81.0	8.27	N/A	26.82	N/A	38.3
G05	266332.0	3965442.0	339.5	G128	IEC	81.0	7.62	N/A	23.36	N/A	33.4
G06	265111.0	3964431.0	340.3	G128	IEC	81.0	9.50	N/A	30.16	N/A	43.1
G07	265183.0	3964678.0	350.0	G128	IEC	81.0	9.37	N/A	29.86	N/A	42.7
G08	265377.0	3964872.0	333.2	G128	IEC	81.0	8.98	N/A	28.95	N/A	41.4
G09	265494.0	3965103.0	336.6	G128	IEC	81.0	8.82	N/A	28.14	N/A	40.2
G10	265706.0	3965298.0	404.2	G128	IEC	81.0	9.37	N/A	29.02	N/A	41.5
G11	265738.0	3966043.0	448.5	G128	IEC	81.0	9.72	N/A	30.39	N/A	43.4
G12	265460.0	3966425.0	383.5	G128	IEC	81.0	9.06	N/A	28.18	N/A	40.3
G13	265423.0	3966679.0	375.0	G128	IEC	81.0	9.71	N/A	30.84	N/A	44.1
G14	258588.0	3963856.0	221.3	G128	IEC	81.0	10.42	N/A	33.85	N/A	48.4
G15	258729.0	3964080.0	236.7	G128	IEC	81.0	9.45	N/A	29.81	N/A	42.6
G16	258842.0	3964323.0	235.7	G128	IEC	81.0	10.08	N/A	32.84	N/A	46.9
G17	258793.0	3964584.0	262.4	G128	IEC	81.0	11.10	N/A	36.43	N/A	52.1
G18	257940.0	3964315.0	270.9	G128	IEC	81.0	11.16	N/A	36.18	N/A	51.7
G19	258052.0	3964750.0	264.4	G128	IEC	81.0	10.95	N/A	35.88	N/A	51.3
G20	258541.0	3965077.0	298.6	G128	IEC	81.0	12.00	N/A	39.20	N/A	56.0

Number of turbine (WEC)	Scale and shape parameter of Weibull function. Based on long term correlated measurement data.		Wake affected scale and shape parameter of Weibull function. Based on long term correlated measurement data.		Wind shear over all direction sectors.	Maximum wind shear per direction sector.	Frequency of referring direction sector	Minimum (e.g. negative) wind shear per direction sector.	Frequency of referring direction sector	Maximum vertical inflow per direction sector (caused by terrain steepness)	Frequency of referring direction sector	Maximum horizontal inflow angle: maximum angle of inflow direction between upper and lower tip height	Frequency of referring direction sector
WEC	**C (A)**	**k**	**C (A) -w-**	**k -w-**	**Wind Shear Exponent (α)**					**Flow Inclination [°]**			
					α_{ave} [/]	**α_{max} [/]**	**frequ. [%]**	**α_{min} [/]**	**frequ. [%]**	**vertical**	**frequ. [%]**	**dir. gradient**	**frequ. [%]**
G01	10.70	1.81	N/A	N/A	0.07	0.39	0.5	0.01	23.1	6.4	20.7	23.1	0.5
G02	9.13	1.64	N/A	N/A	0.18	1.03	0.6	0.03	27.5	7.1	0.6	44.3	0.6
G03	9.85	1.69	N/A	N/A	0.07	0.33	4.6	-0.01	18.4	7.1	0.8	25.6	1.2
G04	9.40	1.66	N/A	N/A	0.10	0.40	0.6	0.03	24.9	12.6	0.6	18.2	12.9
G05	8.42	1.35	N/A	N/A	0.27	0.91	15.3	0.05	1.7	5.9	19.7	13.9	8.2
G06	10.90	1.92	N/A	N/A	0.07	0.35	0.6	0.03	14.8	6.2	5.3	6.7	0.5
G07	10.76	1.92	N/A	N/A	0.08	0.37	0.6	0.03	4.1	2.9	4.1	10.1	0.6
G08	10.29	1.89	N/A	N/A	0.12	0.66	0.6	0.05	4.2	4.2	4.2	22.7	0.6
G09	10.11	1.87	N/A	N/A	0.17	1.26	0.6	0.03	23.2	7.9	0.5	24.5	0.5
G10	10.77	1.90	N/A	N/A	0.17	0.50	13.0	0.03	15.8	6.3	21.9	14.5	18.4
G11	11.18	1.83	N/A	N/A	0.07	0.14	0.5	0.03	1.4	7.3	14.2	11.5	9.4
G12	10.41	1.93	N/A	N/A	0.17	0.45	2.6	0.08	16.9	3.1	0.8	10.1	21.0
G13	11.16	1.92	N/A	N/A	0.09	0.30	3.1	-0.00	3.9	9.1	1.5	5.0	0.5
G14	11.86	1.74	N/A	N/A	0.10	0.34	0.6	0.00	27.0	5.8	1.0	7.2	1.0
G15	10.81	1.94	N/A	N/A	0.12	0.22	0.6	0.05	22.4	4.3	22.4	8.8	3.4
G16	11.52	1.88	N/A	N/A	0.11	0.42	2.9	0.03	21.0	-2.8	2.9	14.2	0.5
G17	12.70	1.89	N/A	N/A	0.06	0.25	3.4	0.01	17.5	4.2	17.5	9.0	11.9
G18	12.79	1.95	N/A	N/A	0.04	0.21	0.6	0.01	27.5	3.8	0.6	8.2	3.3
G19	12.52	1.85	N/A	N/A	0.09	0.42	1.4	0.02	26.2	3.5	14.5	12.0	0.6
G20	13.74	1.85	N/A	N/A	0.09	0.18	15.6	-0.00	20.7	7.3	1.4	7.1	1.0

Number of turbine (WEC)	Distance to the closest turbine given in rotor diameter (RD). [Only necessary if l_{eff} was not calculated.]	Annual average air density on turbine location at hub height [Only necessary if wind speeds are not air density corrected.]	Representative or ~~Characteristic~~ Turbulence Intensity according to >SIAS_SiteVerification-Requirements_Consultant...pdf< however in 2 m/s wind bins.							
WEC	**Distance (RD)**	**d [kg/m³]**	**Representative or ~~Characteristic~~ Turbulence [%]**							
			5 [m/s]	**7 [m/s]**	**9 [m/s]**	**11 [m/s]**	**13 [m/s]**	**15 [m/s]**	**17 [m/s]**	**19 [m/s]**
G01	2.00	1.155	17,0%	14.4%	13.3%	12.5%	11.4%	9.9%	9.3%	8.7%
G02	2.00	1.162	21.9%	19.5%	17.3%	14.3%	11.9%	9.6%	9.3%	9.3%
G03	2.00	1.162	19.2%	16.7%	15.7%	14.1%	12.2%	10.2%	9.1%	9.2%
G04	2.00	1.167	19.1%	16.5%	14.8%	12.5%	10.6%	9.6%	9.2%	8.9%
G05	5.02	1.162	49.1%	32.9%	19.4%	12.5%	11,0%	9.7%	9.8%	9.3%
G06	2.01	1.162	15,0%	12.1%	10.5%	10.4%	9.9%	9.3%	9.1%	8.9%
G07	2.01	1.161	14.9%	12.4%	11,0%	10.6%	10,0%	9,0%	8.8%	8.5%
G08	2.02	1.162	15.5%	13,0%	11.8%	11.2%	10.2%	9.2%	8.8%	8.5%
G09	2.02	1.162	16,0%	13,0%	12,0%	11.3%	10.5%	9.5%	9.5%	9.1%
G10	2.25	1.155	15.5%	12.4%	11.3%	10.9%	10.6%	10,0%	9.9%	9.7%
G11	3.69	1.150	16.1%	13.6%	12.6%	11.9%	11.2%	10.2%	9.6%	9.5%
G12	2.01	1.157	15.6%	13,0%	12.1%	11.5%	11,0%	10.6%	10.5%	10.1%
G13	2.01	1.158	14.8%	12.3%	11.2%	10.6%	10.3%	9.3%	9,0%	8.9%
G14	2.07	1.175	16.1%	13.9%	12.7%	11.9%	10.8%	8.8%	7.8%	6.8%
G15	2.07	1.173	14.9%	12.5%	11.1%	10.5%	9.5%	8.3%	8,0%	7.5%
G16	2.07	1.173	15.5%	12.6%	10.9%	10.4%	10.3%	9.6%	9,0%	8.8%
G17	2.07	1.170	13.7%	10.9%	9.1%	8.6%	8.3%	8.2%	7.8%	7.5%
G18	3.51	1.169	13.6%	10.5%	9,0%	8.4%	8.2%	7.8%	7.6%	7,0%
G19	3.51	1.170	14.5%	11.2%	9.8%	9.5%	9.1%	8.6%	8,0%	7.4%
G20	4.33	1.166	13.8%	10.8%	9.2%	8.5%	8.3%	8.2%	7.7%	7.4%

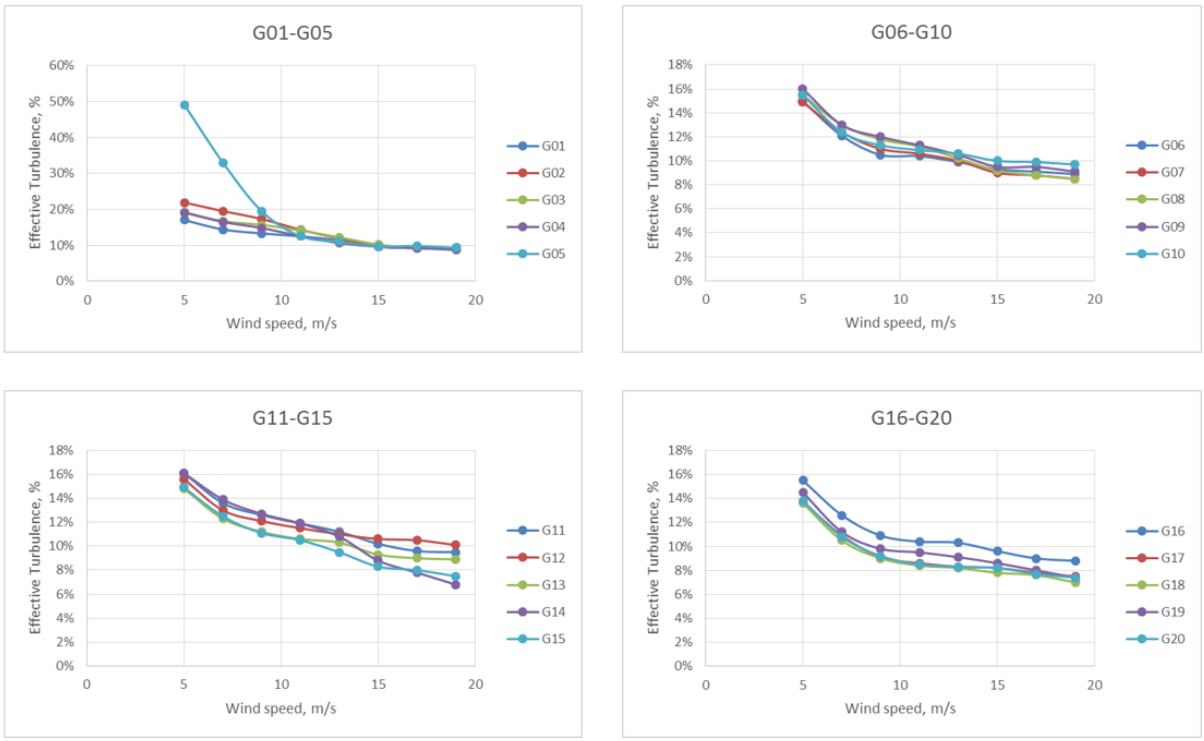

Figure 4.12 Wind speed and Effective Turbulence graphs for all the 20 turbines.

4.13. K-ε vs tke turbulence model

Two turbulence models k-ε and tke were compared. Two cases (run5 and run6 in the Table 4.4) have exactly the same parameters exept turbulence model. Conclusions are listed below:

- K-ε does not disipate with height
- Tke is better in reduction. Turbulence intensity has improve.
- Tke improves Turbulence Intensity with height vs k-ε. This is shown by Figure 4.13 and verfied by cross-cross predictions (Table 4.11 & 4.12). However, no improvement in vertical V_k profiles is observed (Table 4.11 & 4.12)
- Furthermore, tke presents much worse horisontal cross-predictions (Table 4.13)

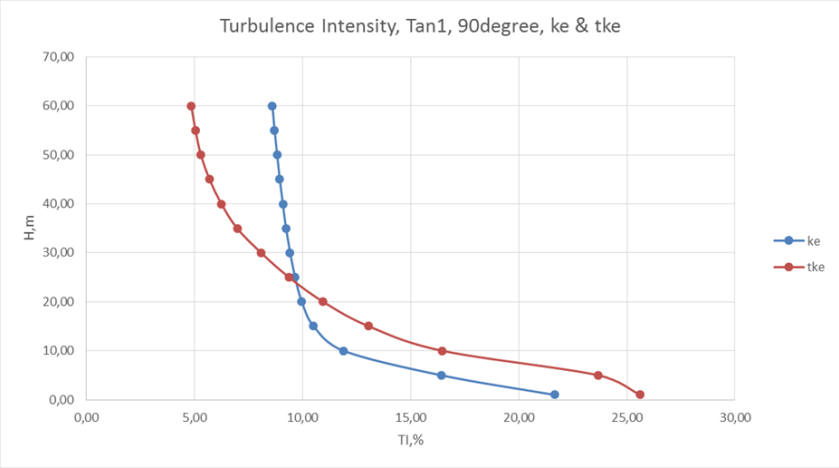

Figure 4.13 turbulence intensity for ke and tke

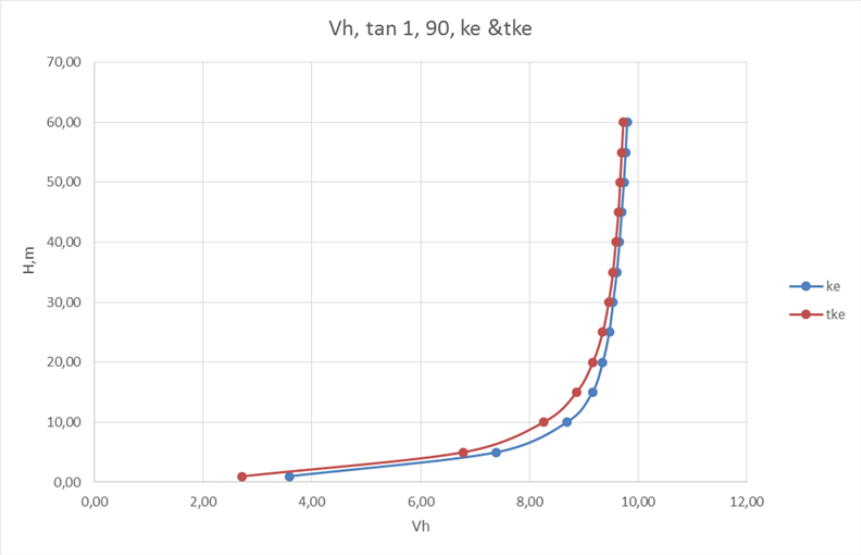

Figure 4.14 Velocity for ke and tke

Table 4.11 – Tke and k-ε turbulence model comparison, vertical cross prediction, TAN1

TAN1, vertical cross-prediction					
		Wind speed [m/s]		TI(V>5) [%]	
From	To	kε error	tke error	kε error	tke error
20TAN1	40TAN1	1,20%	1,74%	1,21%	0,07%
40TAN1	20TAN1	-1,15%	-1,65%	-1,25%	0,00%
20TAN1	60TAN1	3,44%	4,80%	1,31%	0,02%
60TAN1	20TAN1	-3,18%	-4,21%	-1,38%	0,23%
40TAN1	60TAN1	2,18%	2,86%	0,14%	-0,08%
60TAN1	40TAN1	-2,09%	-2,63%	-0,13%	0,12%
RMS		2,37%	3,20%	1,06%	0,11%

Table 4.12 – Tke and k-ε turbulence model comparison, horizontal cross prediction, TAN2

TAN2, vertical cross-prediction					
		Wind speed [m/s]		TI(V>5) [%]	
From	To	kε error	tke error	kε error	tke error
20TAN1	40TAN1	0,08%	0,83%	1,23%	-0,80%
40TAN1	20TAN1	0,02%	-0,69%	-1,35%	0,79%
20TAN1	60TAN1	1,44%	-1,07%	1,52%	-1,07%
60TAN1	20TAN1	-1,16%	-1,36%	-1,78%	1,02%
40TAN1	60TAN1	1,30%	0,86%	0,33%	-0,27%
60TAN1	40TAN1	-1,24%	-0,77%	-0,38%	0,23%
RMS		1,05%	0,96%	1,23%	0,77%

Table 4.13 – Tke and k-ε turbulence model comparison, horisontal cross prediction, TAN1 & TAN2

TAN 1 & TAN2, horisontal cross-prediction					
		Wind speed [m/s]		TI(V>5) [%]	
From	To	kε error	tke error	kε error	tke error
60TAN1	60TAN2	2,88%	27,21%	-2,66%	-4,65%
60TAN2	60TAN1	-7,09%	-14,67%	1,77%	3,36%
RMS		5,41%	21,86%	2,26%	4,06%

5. Deviation from advise guidelines

Below are listed the issues encountered during the work on SV study. They are part of usual and advised guidelines for this type of works. Any deviations can be related to quality of input data of some inaccuracies for the studied site. The most relevant limitations are briefly explained below. The impact of deviations is not quantified.

5.1. Concerning wind data

The wind data quality and mast instrumentation are free from errors and are considered to be of good quality. The wind data was supplied so this opinion is made based on data and documentations sent.

5.2. Concerning CFD modelling

The CFD model for final case did not present abnormal numerical behaviour. All the 12 simulations did converge normally. The only case which did not converge was case for 90^{o} for tke turbulence model. The rest of the cases for tke turbulence model converge normally.

Assessment of wind model performance was carried out from both vertical and horizontal cross-predictions. Both presented good accuracy with RMS error of 2,37% and 3,53% for vertical validations respectively for TAN1 and TAN2 and 3,53% for horizontal validation for 60m for both masts in terms of wind speed. For turbulence intensity the error were even lower: 1,06% (TAN1) and 1,23% (TAN2) for the vertical validations and 1,30% for horizontal validation.

The possibility of verifying the ability of the model by vertical and horizontal cross-prediction give certainty to the model performance.

5.3. Concerning Wake turbulence modelling

It should be noted that the wake of wind turbines was not considered in this work. Even if the wake turbulence would be added the limit would not be exceeded.

6. Final Remarks

The Site Verification study for Tanger Wind farm was successfully concluded and all the major IEC and SV parameters were estimated.

The analysis of wind farm layout was carried out with data from two masts (TAN1 and TAN2) for 3 heights above the ground: 20 m, 40 m, and 60 m.

Estimates were obtained using WINDIE™, a CFD software designed for wind energy industry for atmospheric flow modelling.

Model performance was accurate for the terrain complexity. It was assessed using the available local observations. In terms of wind speed and turbulence intensity the model was truthful. The possibility of extrapolating the model both vertically and horizontally cause that the model become very reliable.

- Vertical cross predictions had a RMS error of 2,37% (TAN1) and 3,53% (TAN2) in wind speed and 1,06% (TAN1) and 1,23% (TAN2) in ambient turbulence intensity.
- Horizontal cross prediction had a RMS error of 3,53% in wind speed and 1,30% in ambient turbulence intensity.

The values of following parameters received from Site Verification Study:

- **Average wind speed for nearly all turbines and some even above Wind Class IA** of 10m/s. Of these the most critical is G20 with 12m/s
- **Average wind shear value above the upper limit at a single layout position, G05** with value of 0.27, the rest values do not exceed the limit
- **Flow inclination value for two turbines positions above the limit:** G04 with 12,6 and G13 with 9.1
- **Effective turbulence values were below the nominative limit** of 18% for subclass A turbines at 15m/s for each turbine.
- **No other site assessment issues were observed** for any other turbine.

Appendix

I References

[1] Burton T.. Shape D.. Jenkigns N.. Bossanyi E.. 'Wind Energy Handbook". 2001

[2] Manwell J.F.. McGowan J.G.. Rogers A.L.. "Wind Energy Explained. Theory Design and Application". 2002

[3] Amendment 1, IEC 61400-1. "Wind turbines Part 1: Design Requirements". ed. 3. 2010

[4] IEC 61400-1. "Wind Turbines Part 1: Design Requirements". ed. 3.2005

[5] IEC 61400-1. "Wind Turbine Generator Systems Part 1: Safety Requirements". ed. 2. 1999

[6] Castro. F.A.. Palma. J.M.L.M.. Silva Lopez. A. "Simulation Of The Askervein Flow. Part 1: Reynolds Averaged Navier-Stokes Equations (k-ε Turbulence Model)".2003

[7] Castro F.A.. Silva Santos C.. Costa J.C.. "Development of a meso-microscale coupling procedure for a site assemsment in complex terrain". EWEC 2010 Proceedings

[8] "Surface meteorology and Solar Energy (SSE) Release 6.0 Methodology, Version 3.0" NASA, November 15, 2016, http://eosweb.larc.nasa.gov/PRODOCS/sse/table_sse.html